GCM SIMULATIONS OF THE MARTIAN WINTER POLAR ATMOSPHERE AND CO_2 SNOWFALLS: DEPENDENCE OF HORIZONTAL RESOLUTION AND RADIATIVE EFFECTS OF CO_2 ICE CLOUDS.

T. Kuroda[1], [1]Department of Geophysics, Tohoku University (6-3 Aramaki-aza-Aoba, Aoba, Sendai 980-8578 Japan, tkuroda@tohoku.ac.jp).

Introduction: In the winter polar atmosphere of Mars, the warming of upper atmosphere occurs due to the adiabatic heading enhanced by the Hadley cell [1,2]. With a solstitial global dust storm, the warming becomes even stronger [3]. Also, the seasonal CO_2 polar cap is formed by the CO_2 ice particles which are formed in the atmosphere and falls on the surface, as well as the CO_2 ice condensed directly on the surface. We have reproduced that the CO_2 snowfalls in northern winter polar atmosphere were strongly modulated by the cold phases of transient baroclinic waves, making the snowfalls rather periodic, and also that the accumulation of the snowfalls had spatial dependences using a Mars Global Climate Model (MGCM) [4]. In this presentation, further MGCM investigations about the properties of the winter polar atmosphere and CO_2 snowfalls on Mars, especially about the dependence of horizontal resolution and radiative effects of CO_2 ice clouds, will be shown.

Model description: The DRAMATIC (Dynamics, RAdiation, MAterial Transport and their mutual InteraCtions) MGCM used in this study has been developed on the dynamical core of CCSR/NIES/FRCGC MIROC with a spectral solver for the three-dimensional primitive equations [5]. For the application to Mars, radiative effects of gaseous CO_2 and airborne dust has been implemented as well as realistic surface parameters (topography, albedo, thermal inertia and roughness) [6].

A simple scheme representing the formation and sedimentation of CO_2 ice clouds has been implemented into the MGCM, in which we assume the particle size of CO_2 ice clouds to be ~50 μm near the surface [4]. The formed clouds can be transported also by advection. The definition of the spatial dust distribution is based on the MY26 dust scenario [7] and traditional assumption of vertical profile [8]. The non-LTE effect is not considered in the radiative effects of CO_2 molecules.

Three kinds of horizontal resolution are set for the MGCM simulation; T21 (or 5.6° × 5.6° grid interval), T63 (1.9° × 1.9°) and T106 (1.1° × 1.1°). The vertical grid consists of 53 σ-levels with the top of the model at ~90 km.

Sensitivity of the horizontal resolution: Figure 1 shows the 30-sols (L_s=270°-289°)-averaged zonal-mean temperature and CO_2 ice cloud mixing ratio for T21, T63 and T106 simulations. As seen, the polar warming becomes stronger with higher resolution, due to the enhancement of northward wind velocity by the resolved gravity waves in the model [9]. The distributions of the mean amount of CO_2 ice clouds differ between T21 and T63, while they are similar between T63 and T106, possibly due to the change of the mean structure of temperature. Note that the quantitative cloud amount in the upper atmosphere might not realistic because the model does not include a non-LTE parameterization of the cooling by CO_2 molecules, which should result in the overestimation of cooling.

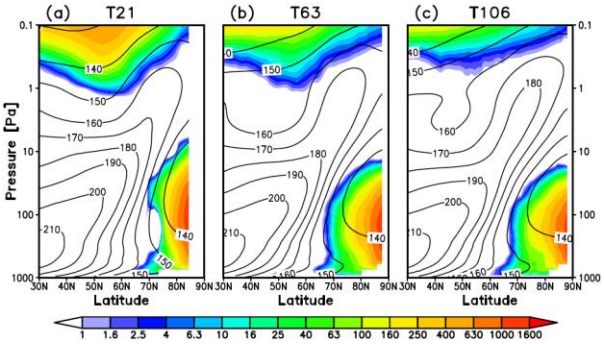

Figure 1: Latitude-altitude cross-sections of zonal-mean temperature (in K, contour) and mixing ratio of CO_2 ice clouds (in ppm of mass, shades) averaged in L_s=270°-289° (30 sols) for (a) T21, (b) T63 and (c) T106 simulations.

Figure 2 shows the north polar projections of mean CO_2 ice cloud mixing ratio at 50 Pa (~25 km altitude) and accumulation rate of surface CO_2 ice in winter (for the same period as in Figure 1). Signals of CO_2 ice clouds are seen only in the north of ~70°N, while the CO_2 ice accumulation is seen in the north of ~55°N, which shows that the formation of seasonal CO_2 ice cap in 55°-70°N is mostly due to the direct condensation on the surface. The amount of CO_2 ice clouds and surface CO_2 ice accumulation are larger in T21, in comparison with T63 and T106 simulations. In the polar atmosphere the kinetic and potential energy due to the harmonics of total wavenumber $21 \leq s \leq 60$, which are resolved in T63 but not resolved in T21, tend to dominate [10]. It is a possible reason for the discrepancy, and further investigations about the effects of those harmonics would be shown in the presentation.

In the T63 and T106 simulations, the distribution of mean CO_2 ice clouds at 50 Pa has the structure of

zonal wavenumber 1 with the peak of ~120°E (as indicated also in Fig.2a of [4]). The peak longitudes of the surface accumulation differ from that, possibly due to the vertical differences of peak temperature induced by stationary planetary waves (see also Fig.3 of [4]). The simulated structures in T63 and T106 are similar, but T106 reproduces also smaller features. In the presentation, results of the southern winter polar region and comparisons with those of the northern polar region (displayed here) will also be shown.

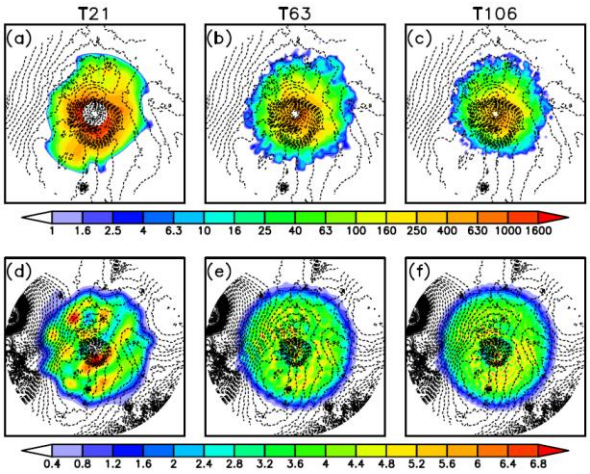

Figure 2: Polar projections (0° longitude at the bottom) of CO_2 ice distributions for the northern polar region averaged in L_s=270°-289° (30 sols). The left (a,d), center (b,e) and right (c,f) columns show the results of T21, T63 and T106 simulations, respectively. Shades represent (a-c) the mixing ratio of CO_2 ice clouds (in ppm of mass) and (d-f) the accumulation rate of surface CO_2 ice (in kg m^{-2} sol^{-1}). Dotted contours represent the topography. The edge latitudes of the plots are 60°N for (a-c) and 40°N for (d-f).

Sensitivity of the radiative effects of CO_2 ice clouds: Figure 3 shows the preliminary results of the longitude-altitude cross-sections of 3-sols-averaged temperature and CO_2 ice cloud mixing ratio at ~80°N and L_s~280° in T21, comparing between the results of radiatively-passive and active CO_2 ice clouds. The refractive index of CO_2 ice clouds is taken from [11] for the radiatively-active calculation. Note that only the infrared radiation should be effective because of the polar night.

As seen, with the radiatively-active clouds, the atmospheric temperature decreases in a few Kelvins, and correspondingly the cloud thickness becomes ~10 times larger than the radiatively-passive cloud case. Note that the results are still preliminary, so further investigations and updated results would be shown in the presentation.

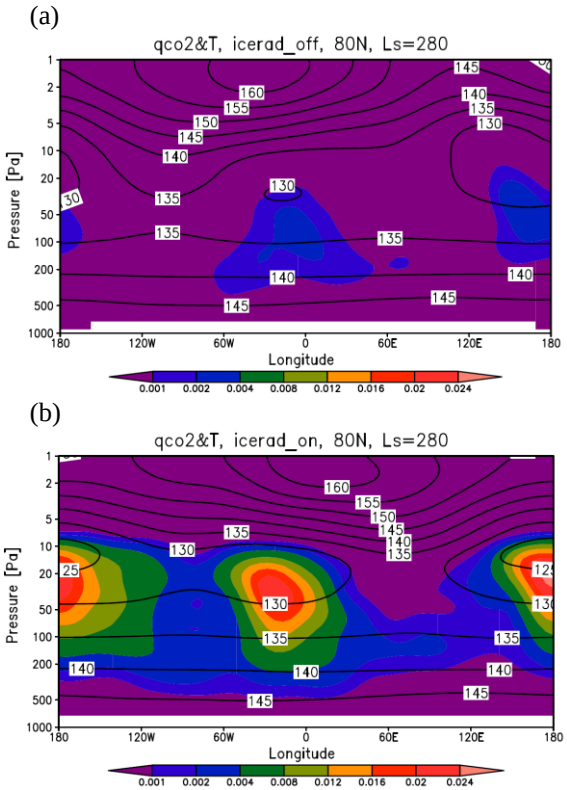

Figure 3: Longitude-altitude cross-sections of 3-sols-averaged temperature (in K, contour) and mass mixing ratio of CO_2 ice clouds (shades) at ~80°N and L_s~280° with T21 horizontal resolution, for (a) radiatively-passive and (b) radiatively-active CO_2 ice clouds.

References: [1] Heavens, N.G. et al. (2011) *JGR, 116*, E01010. [2] Medvedev, A.S. and Hartogh, P. (2007) *Icarus, 186*, 97–110. [3] Kuroda, T. et al. (2009) *J. Meteor. Soc. Japan, 87*, 913–921. [4] Kuroda, T. et al. (2013) *GRL, 40*, 1484–1488. [5] K-1 Model Developers (2004) *K-1 Tech. Rep., Univ. of Tokyo, 1*, 1–34. [6] Kuroda T. et al. (2005) *J. Meteor. Soc. Japan, 83*, 1–19. [7] Montabone, L. et al. (2015) *Icarus, 251*, 65–95. [8] Conrath, B.J. (1975) *Icarus, 24*, 36–46. [9] Kuroda, T. et al. (2015) *GRL, 42*, 9213–9222. [10] Kuroda, T. et al. (2016) *JAS, 73*, 4895–4909. [11] Warren, S.G. (1986) *Appl. Opt., 25*, 2650–2674.